GEANT4 simulations of the n_TOF spallation source and their benchmarking

13 authors, including:

Cristian Massimi
University of Bologna
208 PUBLICATIONS   **862** CITATIONS

N. Colonna
INFN - Istituto Nazionale di Fisica Nucleare
404 PUBLICATIONS   **3,688** CITATIONS

C. Guerrero
Universidad de Sevilla
229 PUBLICATIONS   **940** CITATIONS

Davide Mancusi
Atomic Energy and Alternative Energies Com…
97 PUBLICATIONS   **539** CITATIONS

Some of the authors of this publication are also working on these related projects:

Project — Neutron capture cross-section of 155,157Gadolinium View project

Project — Geant4 simulations of the n_TOF spallation target View project

GEANT4 simulations of the n_TOF spallation source and their benchmarking

S. Lo Meo, M.A. Cortés-Giraldo, C. Massimi, J. Lerendegui-Marco,
M. Barbagallo, N. Colonna, C. Guerrero, D. Mancusi, F. Mingrone,
J.M. Quesada, M. Sabate-Gilarte, G. Vannini, V. Vlachoudis
and The n_TOF Collaboration

Special Article – Tools for Experiment and Theory

GEANT4 simulations of the n_TOF spallation source and their benchmarking

S. Lo Meo[1,2,a], M.A. Cortés-Giraldo[6], C. Massimi[2,3], J. Lerendegui-Marco[6], M. Barbagallo[4], N. Colonna[4], C. Guerrero[6], D. Mancusi[5], F. Mingrone[2], J.M. Quesada[6], M. Sabate-Gilarte[6,7], G. Vannini[2,3], V. Vlachoudis[7], and The n_TOF Collaboration[b]

[1] ENEA, Research Centre "Ezio Clementel", I-40129 Bologna, Italy
[2] INFN, Section of Bologna, I-40127 Bologna, Italy
[3] Physics and Astronomy Dept. "Alma Mater Studiorum" - University of Bologna, I-40126 Bologna, Italy
[4] INFN, Section of Bari, I-70125 Bari, Italy
[5] CEA-Saclay, DEN, DM2S, SERMA, LTSD, F-91191 Gif-sur-Yvette CEDEX, France
[6] Universidad de Sevilla, Facultad de Física, 41012 Sevilla, Spain
[7] European Organization for Nuclear Research (CERN), CH-1211 Geneva, Switzerland

Abstract. Neutron production and transport in the spallation target of the n_TOF facility at CERN has been simulated with GEANT4. The results obtained with different models of high-energy nucleon-nucleus interaction have been compared with the measured characteristics of the neutron beam, in particular the flux and its dependence on neutron energy, measured in the first experimental area. The best agreement at present, within 20% for the absolute value of the flux, and within few percent for the energy dependence in the whole energy range from thermal to 1 GeV, is obtained with the *INCL++* model coupled with the GEANT4 native de-excitation model. All other available models overestimate by a larger factor, of up to 70%, the n_TOF neutron flux. The simulations are also able to accurately reproduce the neutron beam energy resolution function, which is essentially determined by the moderation time inside the target/moderator assembly. The results here reported provide confidence on the use of GEANT4 for simulations of spallation neutron sources.

1 Introduction

Spallation neutron sources are gaining increasing importance for their impact on several fields of basic and applied nuclear physics. The wide research area in which spallation neutron beams can be very useful include measurements of cross sections of neutron-induced reactions for Nuclear Astrophysics [1] or for the design of new systems for energy production or nuclear waste incineration [2], material analysis, studies of biologic systems, etc. Several spallation neutron sources are already operational around the world (such as LANSCE at Los Alamos National Laboratory, USA, the Spallation Neutron Source in Oak Rigde [3], USA, the n_TOF [4] facililty at CERN, the ISIS [5] facility of Rutherford Appleton Laboratory, UK, the Materials and Life Science Experimental Facility (MLF) at J-PARC [6], Japan) and more are in the phase of construction, such as the European Spallation Source (ESS) [7], or the China Spallation Neutron Source (CSNS) [8].

One of the main challenges for the construction and exploitation of spallation neutron sources is related to the simulation of the neutron beam. In most applications it is of fundamental importance to accurately know the neutron flux, or at least its dependence on the neutron energy, as well as other features like the spatial beam profile, the contamination of charged particles and γ-rays in the beam, and related background. In time-of-flight (TOF) facilities it is also of crucial importance to know with good accuracy the so-called resolution function, *i.e.* the time distribution of neutrons emerging from the target with a given energy. While measurements can be performed for all these quantities, most often they are incomplete, covering a portion of the energy region, or may not reach the level of accuracy or resolution required. Furthermore, simulations are important in the design phase of a new spallation facility, as they can supply a wealth of information on the expected features of the neutron beam. In this case it is important to count on reliable, previously validated Monte Carlo (MC) tools. In this respect, the most accurate and widely used Monte Carlo

[a] e-mail: sergio.lomeo@enea.it
[b] www.cern.ch/ntof.

codes are MCNP [9] and FLUKA [10]. The latter has been successfully used to simulate the characteristics of the neutron beam at the n_TOF facility. These simulations have been validated against the experimental results on the flux and energy resolution function of the neutron beam, showing a good agreement and allowing to extract information otherwise not accessible, such as the moderation time, which affects the reconstructed neutron energy from the measured TOF. A slight drawback of this program is the use of group cross sections below 20 MeV neutron energy, which limits the achievable energy resolution of the simulated neutron flux. Another MC tool that could in principle be used for the simulation of spallation neutron sources is GEANT4 [11], the widely used simulation toolkit developed at CERN. However, as of now few studies have been performed on the accuracy that can be reached in the prediction of the neutron beam characteristics at spallation facilities, with this tool. In particular, while the high-precision model based on evaluated cross sections can safely be used for the transport of neutrons of energy below 20 MeV (see, for example, ref. [12]), no systematic study has been performed on the high-energy model or models, among the various ones available, that best reproduce the spallation neutron production in the full energy range. In order to address this important issue, we have performed GEANT4 simulations of the neutron beam characteristics of the n_TOF facility at CERN. Different high-energy models have been tested in order to identify the most appropriate one, on the basis of the comparison between the simulated and measured features of the neutron beam in the first experimental area of n_TOF.

The paper is organized as follows: in sect. 2 the geometry and material of the spallation target and the physics list (PL) used in the simulations are described, with particular emphasis on the one that best reproduces the neutron beam characteristics of n_TOF. A thorough comparison of the simulation with the features measured in EAR1, in terms of energy-dependent flux, beam profile, resolution function, is presented and discussed in sect. 3. Conclusions are given in sect. 4.

2 GEANT4 simulations

One of the aims of this work is to benchmark GEANT4 simulations of the spallation neutron production against measured characteristics of the n_TOF neutron beam. A detailed description of the facility can be found in ref. [13]. In brief, the facility is based on the spallation of 20 GeV/c protons impinging on a massive lead target. Two spallation targets have been used so far at n_TOF: the first one, an approximately cubic Pb volume, was replaced in 2008 by a cylindrical one, with the additional feature of separated cooling and moderation circuits. The simulations reported here are done for the second target, currently being used. Since its installation, several measurements have been carried out in order to characterize the neutron beam, in terms of neutron flux, beam profile, resolution function and contamination of the beam [13,14].

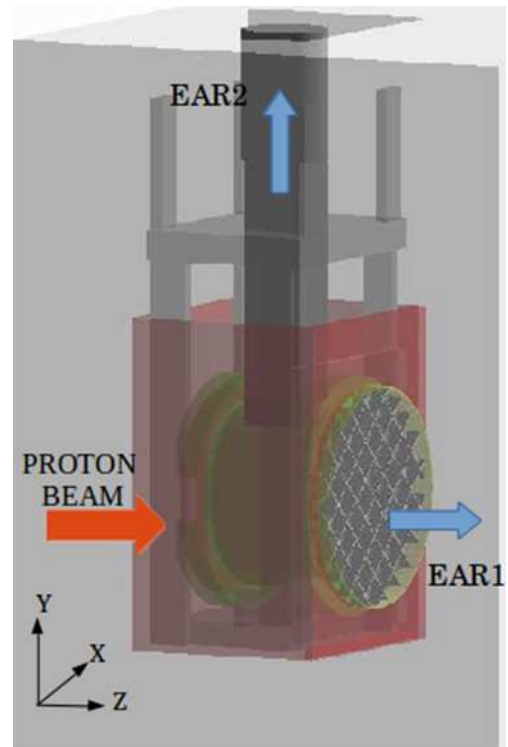Up to recently, only one neutron flight path and the corresponding experimental area were available at n_TOF.

Fig. 1. View of the spallation target, support structures and concrete pit at n_TOF as implemented in GEANT4 simulations.

This measuring station, referred to hereafter as EAR1, at the end of a 185 m long horizontal beam line was complemented in 2014 with a new vertical beam line together with a second experimental area (EAR2). The new beam line is 20 m long, resulting in a much more intense neutron flux but poorer resolution on the reconstructed neutron energy. The simulated features of the neutron beam in EAR2 will be the subject of a forthcoming paper [15].

In order to accurately simulate the n_TOF neutron beam, a realistic description of the geometry and materials of the spallation target and moderator have to be implemented in the MC simulation. The second important ingredient of the simulation is a suitable choice of the PL. In the following, details on spallation target and on the PL used in this work are provided. The implementation of the spallation target and the propagation of the emitted neutrons to the experimental area were performed by two groups, so to avoid possible biases related to details in the geometrical or material description of the target and to the propagation procedure. The results were found to agree within a few percent, thus providing a high level of confidence on the reliability of the simulations.

2.1 The spallation target

The simulated set-up, *i.e.*, the spallation target, the support structures and the concrete pit in which it is mounted, is displayed in fig. 1, while fig. 2 shows in more detail the different elements of the spallation target assembly implemented in the code. The target can be
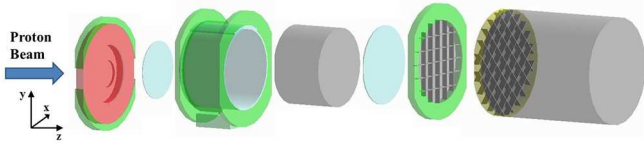
Fig. 2. Exploded-view of the various elements of the n_TOF spallation target implemented in the simulations.

described as made of three main parts placed along the Z-axis. The first part (hereafter referred to as *Front*) corresponds to the area where the protons impinge on the target assembly. The second part (*Target*) is the Pb target itself, with pure cooling water (1 cm layer) in an aluminium container. An opening on the top of this region leads to the second experimental area. Finally, the third part (*End*) is the area where the neutrons are further moderated (by 4 cm layer of pure or borated water) before they enter the beam line towards the first experimental area. The materials and geometry implemented in the simulation reproduce in great detail the ones actually used in the n_TOF spallation target.

The *Front* volume, representing the proton entrance window, is a cylinder, made of an aluminium alloy, known as AW5083, made of 93.35% Al, 4.5% Mg and 7 other elements from Si to Zn. The main part, with outer and inner radius of 35 cm and 20 cm, respectively, and a length of 10 cm, contains cooling water.

The *Target* part is composed of the spallation volume, made of Pb, surrounded by a layer of water, all inserted in the aluminum alloy container. The Pb block is a cylinder 30 cm in radius and 40 cm in length. It is made of a lead alloy with 99.974% Pb and traces of 37 chemical elements ranging from Li to U. The cooling water around the spallation volume, which acts also as moderator of the neutron spectrum, is on average 1.4 cm thick, except on top of the Pb volume, where it is around 3 cm in order to provide additional moderation for the vertical path leading to EAR2. On the bottom part of the target, a series of aluminium guides, 4 mm thick spaced by 4.5 cm, are inserted in the water region, to maintain a constant, forced circulation of water around the Pb cylinder and to reduce the target creep. The cylindrical container, made of AW5083 previously defined, has inner and outer radii of 31.4 cm and 35 cm. In the *End* part of the spallation target, an additional 4 cm thick layer of borated water is used to further moderate neutrons emitted towards EAR1. The borated water contains 4.2 weight% of H_3BO_3, with a ^{10}B enrichment of 95%. This additional moderator is enclosed between two AW5083 sheets 3 mm thickness, reinforced by an internal grid consisting of 10×10 cm^2 0.55 cm thick AW5083 horizontal and vertical bars.

Before entering the 185 m long vacuum tube towards EAR1, neutrons emerging from the spallation target have to cross an air gap of 2.8 cm, and a window, made of 1.6 mm AW5083 sheet reinforced by a grid, rotated by 45° around the Z-axis, similar to the one previously described. Neutrons emitted towards EAR1 are recorded on a tally surface positioned at a distance of 3 cm from the last window, along the Z-axis. Neutrons are recorded if they are emitted in a cone of 10 degrees aperture around the Z-axis.

Besides the *Front*, *Target* and *End* volumes, additional elements outside the spallation target were included in the geometry by one of the groups working on the simulations (see fig. 1). They include a holding structure with six legs made of a aluminium alloy, knows as AW6082, that surrounds the target and has a handle on top that allows hoisting the target from above. The top of this holder features a gap through which the beam line going to EAR2 is connected. Finally, the contention pool surrounding the target assembly, the supporting stainless steel pillar with a diameter of 400 mm, and the concrete bunker (inner volume of $160 \times 205 \times 120$ cm^3, with the EAR1 exit face made of calcite instead of concrete) have also been implemented in the simulated geometry. The composition of the concrete includes Si(23%), O(60%), H(10%) and three other impurities.

2.2 The physics list

GEANT4, version 10.1, offers a wide variety of models for handling physical processes within different energy ranges. Spallation reactions, causing the emission of a large number of nucleons and fragments, are described as a two-step process: intra-nuclear cascade and subsequent de-excitation.

Among the hadronic PLs provided by GEANT4, one that realistically describes both stages has to be found. The inelastic interaction of high-energy protons can be described by the Fritiof [16,17] model *FTFP*, which is used in GEANT4 for simulating the interaction of mesons, nucleons and hyperons in the 3 GeV–100 TeV energy range, and of anti-nucleons, anti-hyperons and anti-nuclei for all energies.

In a recently published work by Lo Meo and collaborators [18], the Liège Intra-nuclear Cascade model *INCL++* [19,20] has been used to study thin-target fission yields. Extensive benchmarks have shown the *INCL++* model has a very good predictive power for the observables related to neutron production in spallation reactions, such as multiplicities and double-differential spectra [21]. The stand-alone version of *INCL++* used in [18] has been coupled with the new version of the *ABLA* model [22], recognized as one of the best de-excitation models by the IAEA Benchmark of Spallation Models [23]. This combination has been proven to yield very accurate predictions for double-differential neutron spectra on pre-actinides at intermediate energies [23,24]. In GEANT4 v10.1 the Liège Intra-nuclear Cascade model has been recently extended to handle reactions between 3 and 15 GeV incident energy [20,25,26]. By default, it is coupled with the native de-excitation model [27] *G4ExcitationHandler*. However, it is possible to couple *INCL++* with an older version of *ABLA* (version 3.0) [28]. In this work, simulations of the n_TOF neutron beam have been performed with both the native de-excitation model and with the old *ABLA* version.

Reactions induced by neutrons with energies smaller than 20 MeV are in all cases simulated by means of the *G4NeutronHP* model, which uses the evaluated data libraries ENDF/B-VII.0 [29] and ENDF/B-VII.1 [30]. An

extensive validation work has been performed by Mendoza *et al.* [31] on the transport of low-energy neutrons with GEANT4.

In order to include in a single PL all the choices described above for the nucleon interactions, the intranuclear cascade, and the de-excitation, we have used the $FTFP\_INCLXX\_HP$ list [32,33], with a minor modification concerning the value of the neutron tracking cut [33], set to 4.0 ms instead of the default value of 10 μs. As will be shown in sect. 3, the choice of the $INCL++$ coupled to either the default de-excitation model in GEANT4, or to the old $ABLA$ model reproduces quite accurately the characteristics of the n_TOF neutron beam, in particular the neutron flux. In fact, this choice provides the best results when compared with other options for the inelastic scattering ($QGSP$) [33] and cascade models ($BERT$ or BIC) [33], especially for the energy dependence of the neutron flux, and its absolute value.

The output of the simulation consists of a large amount of detailed information, *i.e.*, position, direction, momentum, energy, moderation time, for each neutron that crosses the tally surface.

2.3 Optical transport to EAR1

Neutrons produced in the interaction of the proton beam with the spallation target are followed and tracked up to the tally surface positioned at the entrance of the vacuum beam pipe. For a consistent comparison with the experimental data, neutrons need to be propagated to the experimental area. The neutron transport along the beam line to the measuring station approximatively 185 m from the target cannot be efficiently performed by MC simulation since the solid angle subtended by the collimators is extremely small, approximately 7×10^{-9} sr for EAR1. A different procedure has therefore to be used. We remind that from the GEANT4 simulations, neutrons crossing the tally surface are recorded with their position, direction, energy, and moderation time. This last parameter, defined as the time interval between the entrance of the proton beam in the lead target and the arrival time of the secondary particle on the tally surface is important for reconstructing the neutron energy in the same way as in the real measurement, where the total neutron TOF is used. Furthermore, it is fundamental to determine the resolution function of the neutron beam, which is defined as the spread in time of flight of neutrons of a given energy (or vice versa).

The procedure applied in this work consists in geometrically propagating through the beam line, *i.e.* through a software replica of the two collimators installed at n_TOF, a large number of "resampled" neutrons. In particular, for each neutron registered on the tally surface, a constant, large number of new neutrons are generated with the same energy and position as the original one, but with a randomly chosen direction, up to a given maximum angle θ_{MAX}. Both the number of "resampled" neutrons and θ_{MAX} are suitably chosen, the first one in order to obtain a reasonable statistics at the end of the propagation through the beam line, the second one slightly larger than the angle subtended by the first collimator, considering the finite
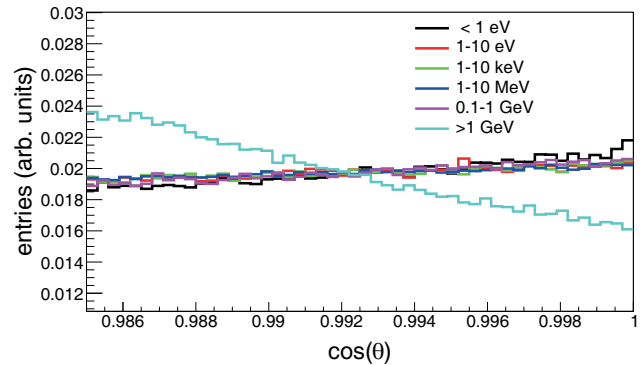

Fig. 3. Distribution of neutron directions along the beam axis toward EAR1, recorded on the tally surface in GEANT4 simulations, for different neutron energies.

dimension of the spallation target. In this work, the limiting angle used for re-sampling is around 0.2 degrees. The procedure of resampling, with random direction, the simulated neutron distributions recorded on the tally surface can be applied only in the assumption that neutrons are emitted isotropically from the spallation target, within a relatively small angle. As shown in fig. 3, this condition is met for simulated neutrons, within a few degree emission angle, for all neutron energies except the highest ones (above 1 GeV), thus justifying the choice of randomly reassigning the neutron polar and azimuthal angle in the resampling procedure.

The "resampled" neutrons are geometrically propagated through the collimation system (see ref. [13] for details on the geometry and composition of the two collimators). For each secondary neutron, the trajectory is calculated according to its position on the tally surface and the randomly generated emission angle. If the neutron does not pass through the collimators placed along the beam line, it is discarded. In the calculation of the trajectory the effect of gravity is taken in consideration, although its effect is negligible for all but thermal (and sub-thermal) neutrons. This simple geometrical propagation does not take into account the effect of neutron scattering in the collimators, which results in a background in the flux measured in EAR1. However, it has been verified experimentally that such a background is small [14], and can be safely neglected in the present analysis. Figure 4 shows the simulated neutron spatial distribution on the tally surface before (upper panel) and after (lower panel) applying the propagation procedure described above. As evident from the comparison, the effect of the collimation system is to select neutrons mostly emitted from the central region of the spallation target, with the area of emission sensibly smaller than the target dimension. This effect is particularly important for the study of the resolution function of the neutron beam. It also affects the energy distribution of neutrons reaching the experimental area, enhancing the high-energy component which has a sharper spatial distribution centred just a few centimetres off the centre of the spallation target (due to the 10 degrees inclination of the proton beam relative to the entrance surface of the target).
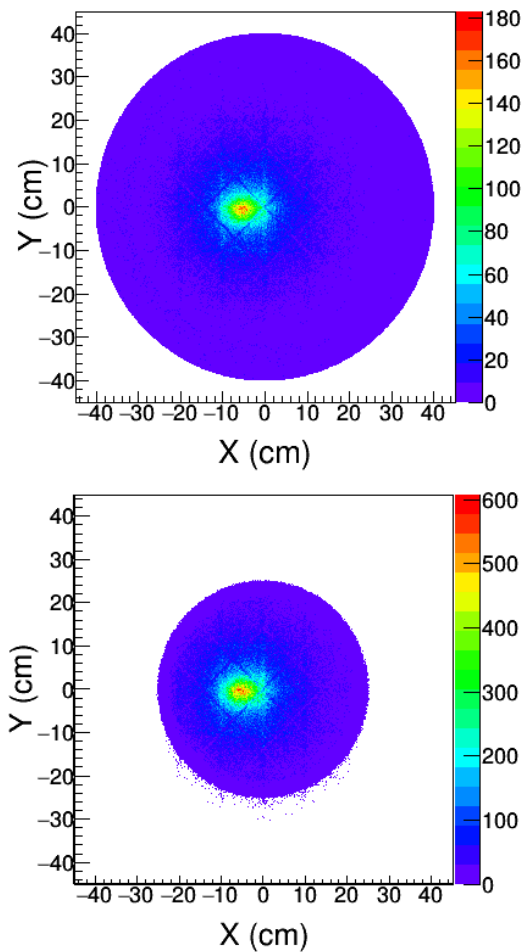
Fig. 4. Spatial distribution of neutrons scored in GEANT4 simulations on the tally surface placed at the entrance of the beam pipe (top panel), and for neutrons reaching EAR1 after geometrical propagation (bottom panel). As evident from the comparison, the collimation system leads to a reduction of the effective source size, since only neutrons emitted from the central region of the spallation target reach the experimental area. This effect has important consequences in particular on the resolution function.

Another important aspect of the propagation is the determination of the neutron energy in the experimental area on the basis of the neutron TOF, by means of a reconstruction procedure consistent with the experimental one. To this end, the simulated moderation time defined above is added to the time needed by the neutron to travel from the tally surface to the experimental area, calculated on the basis of its real energy. A further spread of 7 ns (σ) is considered in the analysis to account for the time width of the real proton beam. The resulting total TOF is then used to determine the reconstructed neutron energy. A further observable determined after the neutron propagation is the spatial beam profile in the experimental area as a function of neutron energy.

In the following, the simulated flux, resolution function and spatial profile of the neutron beam in EAR1 are compared with the ones experimentally determined in recent campaigns. The simulated in-beam γ-ray component is also presented.

3 Results and discussion

The GEANT4 simulations can be benchmarked by comparing the predicted observables with experimental results. From the comparison, one can obtain information on the most appropriate PL for simulating the spallation process. The most important observables are the neutron flux in the experimental area, and in particular its dependence on neutron energy, thermal to 1 GeV, and the resolution function. Another observable is the spatial profile of the neutron beam in the experimental area. All these quantities have been determined with high accuracy in EAR1.

3.1 Neutron flux

To verify the accuracy of the MC simulation, the simulated neutron flux is compared to the experimental flux measured with different detection systems and reactions. For convenience, and consistent with [14], the word "flux" indicates here the total number of neutrons per incident proton pulse, *i.e.* the fluence integrated over the full spatial profile. Details on the measured flux in EAR1 can be found in [14]. Hereafter, the measured quantity is referred to as the "evaluated flux", over the neutron energy range from thermal to about 1 GeV. Historically, the proton pulse corresponds to 7×10^{12} protons impinging on the spallation target. Being n_TOF a white neutron source with energies spanning over several orders of magnitude, the flux is conveniently expressed in units of lethargy, *i.e.* the natural logarithm of energy, $\frac{dn}{d \ln E}$.

Figure 5 shows the flux in EAR1 obtained in GEANT4 simulations with different PLs. For comparison, the evaluated flux is also included in the figure. It can be clearly seen that different high-energy models result in different shapes of the flux distribution, in particular at high energies ($E_n > 10$ MeV), and have a sizeable effect on the magnitude of the flux at all energies. In particular, the Bertini cascade model (*BERT*), both within the *FTFP* and *QGSP* PLs, overestimates the evaluated flux, by more than 70%, so one can reasonably conclude that these choices are not adequate for simulating a lead spallation target as neutron source. The binary cascade (*BIC*) and the *INCL* model, with or without *ABLA*, predict a lower flux, more consistent with the experimental results, although the shape of the high-energy part (above 10 MeV neutron energy) seems to be more correct with the *INCL* model. The best agreement between the simulations and the evaluated flux is observed for the *INCL* model coupled with the native de-excitation model of GEANT4. As described in sect. 2.2 the *ABLA* model included in the present version of GEANT4 is relatively old. New features have been introduced in the most recent releases of *ABLA*, like the one used in [18] in conjunction with the *INCL++* stand-alone code, that may have some effect on the generation of neutrons in spallation processes.

The *INCL* model coupled with the native GEANT4 de-excitation code still overestimates the measured neutron flux, by approximately 20%, on average. The origin of this
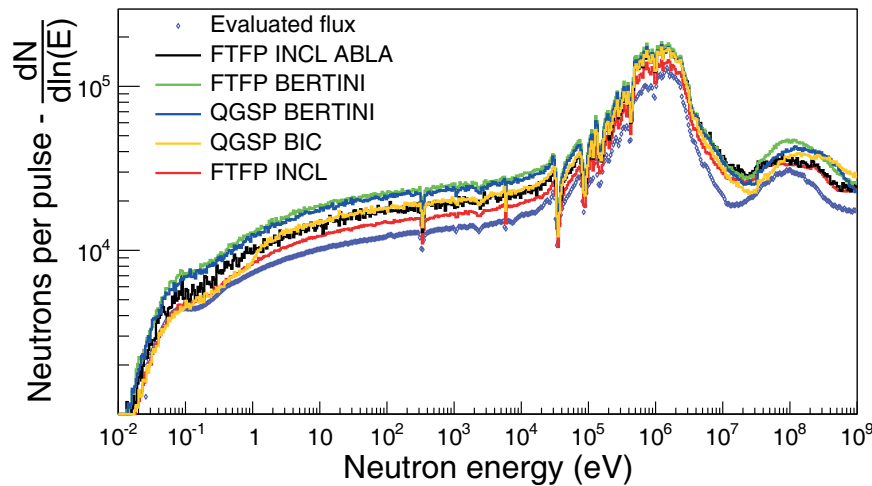
Fig. 5. Total number of neutrons per proton pulse reaching EAR1, simulated with GEANT4 for different combinations of the high-energy interactions and intra-nuclear cascade models. For comparison the measured neutron energy distribution (the so-called "evaluated flux") is also shown in the figure. Except for one case, in which *ABLA* was coupled to *INCL*, in all other simulations the native GEANT4 de-excitation model was used.

difference is most probably related to some features of the intra-nuclear cascade models (as discussed later). Alternative explanations related to the accuracy of the geometry and materials in the simulations, or to the alignment of the collimation system cannot be excluded, although to the best of our knowledge these effects may account only for a few percent difference.

In order to perform a more detailed comparison with the shape of the measured neutron energy distribution, the simulated flux with the *INCL++* model has been re-normalized to the experimental data in the neutron energy region from 10 eV to 10 keV. Figure 6, upper panel, shows the comparison in the whole neutron energy range from 25 meV to 1 GeV. The agreement is in general very good, with just some small difference around 20 MeV and above 100 MeV. The very nice reproduction of the flux shape even in the absorption dips related to the material composition of the spallation target can be appreciated in the bottom panel of fig. 6. The good agreement is obviously due to a realistic description of the target in GEANT4 and, especially, of the high-precision, point-wise, cross sections used in this code for neutron energies below 20 MeV. In fact, it is an important feature of GEANT4 that it allows one to reproduce the neutron flux all the way from thermal to the GeV neutron energy with high accuracy and resolution. We finally remark that, while the simulations based on the *INCL++* model shows the closest agreement on the absolute neutron flux, the other models studied in this work also reproduce the energy dependence of the neutron flux and the high-resolution details, such as the absorption dips.

3.2 Resolution function

A high-quality MC simulation of the spallation source should be able to accurately reproduce the propagation time of neutrons inside the target assembly. We remind

that the stochastic process of moderation inside the Pb target and the moderation system, mostly made of normal and borated water, causes a broadening of the energy distribution of neutrons reaching the experimental area at a given TOF. Such a broadening affects the shape of resonances in the measured cross section, and has to be taken into account when performing a resonance analysis, by means of a suitable resolution function [34, 35]. While this can be studied experimentally by means of some well-known, isolated resonances in the cross section of neutron-induced reactions, a more systematic analysis can only rely on simulations, provided that they are proven reliable. It is worth recalling that the broadening in time introduced by the moderation process strongly depends on the dimensions and materials constituting the neutron-producing target.

A convenient way of expressing the effect of the moderation time is to convert it into an equivalent moderation length, multiplying it by the velocity of the neutron when exiting the spallation target assembly. The distribution of the moderation length simulated with GEANT4 for the n_TOF target is shown as a function of the neutron energy in fig. 7. This 2D plot provides an illustrative overview of the evolution of this effective length with neutron energy. Simulations indicate that beyond a few MeV the time spread of the proton pulse is the main contribution to the response function, with the practical energy limits of the moderation process spanning over nine orders of magnitude, roughly from 100 meV to 100 MeV. In fig. 7 the simulated moderation time was convoluted with the Gaussian distribution of the proton pulse (7 ns RMS). As a side effect the negative distances that can be seen in the upper part of the plot may lead indeed to negative times for fast neutrons escaping from the target in a very short time. If the proton pulse spread is not included in the simulated resolution function, the width of the distribution above a few MeV is much smaller, with
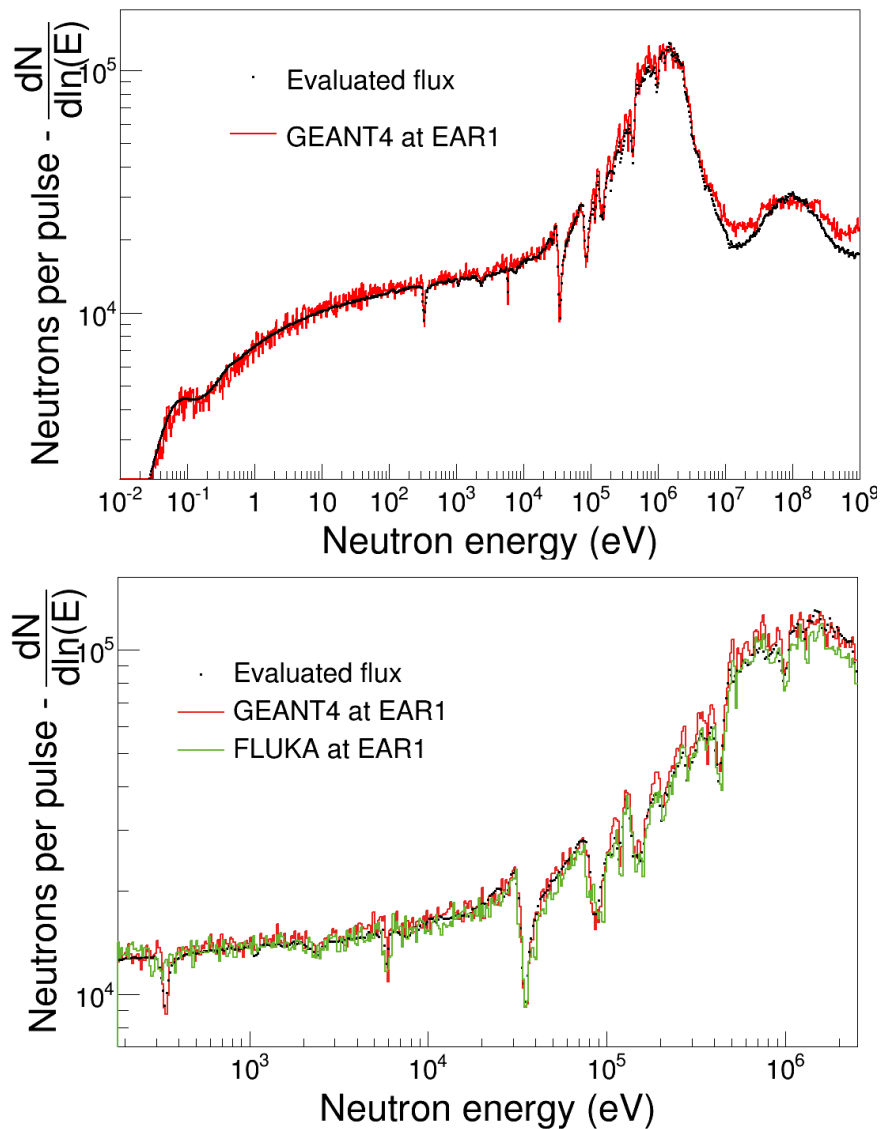
Fig. 6. Top: GEANT4 simulations of the total number of neutrons per pulse reaching EAR1 at n_TOF, compared with the experimental data from [14] (referred to as "evaluated flux"). The simulations have been normalized to the experimental data in the neutron energy region from 10 eV to 10 keV, with a normalization factor of 0.79. Bottom: zoom of the upper plot in the energy region from 200 eV to 3 MeV, for a better visualization of the absorption dips caused by the aluminium windows in the target assembly. For comparison, the FLUKA+MCNP simulations from ref. [14] are also shown in the figure. Similarly to GEANT4, they have been normalized to the experimental data with a normalization factor of 0.77.

the maximum shifting towards higher distances, up to the saturation value for relativistic neutrons of ~ 0.5 m (corresponding to the distance between the entrance of the target and the tally surface).

The projection of fig. 7 for selected neutron energy intervals below 5 MeV, where the effect of the proton pulse spread is not dominant, are shown in fig. 8. It can be seen that in average the simulated moderation distance is roughly constant in a wide neutron energy range, with the maxima located at small values (~ 10 cm). For thermal neutrons the effective length increases slightly and above tens of keV the tails of the distributions extend above 2 m, emphasising the importance of considering the whole bunker as part of the target-moderator assembly. Beyond hundreds of keV, the distribution width decreases and the

position of the maximum is shifted towards larger values. The shape of the simulated moderation length, either parametrized as a function of neutron energy or inserted as a numerical matrix, is used in codes commonly employed for resonance shape analysis, such as SAMMY [36].

In order to confirm the reliability of GEANT4 in predicting the resolution function of the n_TOF neutron beam, a comparison has been performed between the simulated and measured broadening for some selected resonances in the well-known neutron capture cross section of ^{197}Au [37] and ^{56}Fe. The comparison is shown in fig. 9. The very good reproduction of the measured resonance shape provides confidence on the accuracy of the simulated moderation distance, and consequently on the resolution function of the neutron beam.
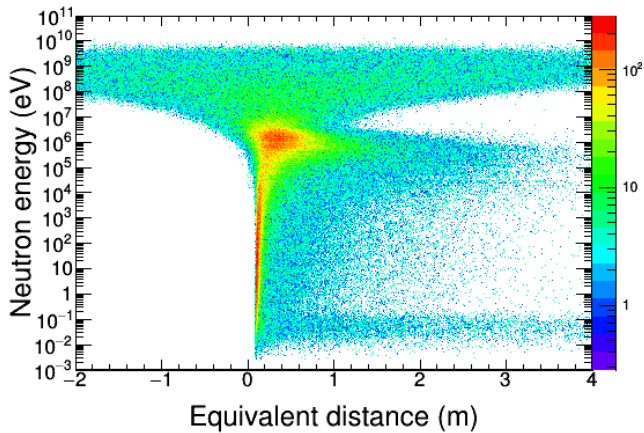
Fig. 7. Probability distribution of the equivalent moderation distance, as a function of neutron energy, obtained from GEANT4 simulations of the n_TOF spallation target. The simulated moderation time was convoluted with the Gaussian distribution of the proton pulse (7 ns RMS) and this time spread is causing the negative values above approximately 10 MeV.
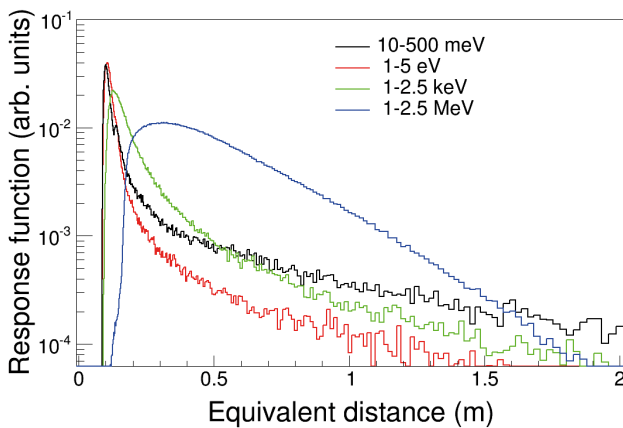

Fig. 8. Projections of fig. 7 for selected neutron energy intervals below 5 MeV, where the effect of the proton pulse spread is not dominant.

3.3 Beam profile

Another characteristic of the neutron beam that can be conveniently simulated is its spatial profile in the experimental area. This information is required for measurements with samples smaller than the beam. In this case, it is important to accurately determine the fraction of the neutron beam impinging on the sample, also called "beam interception factor" (BIF), and its dependence on neutron energy. The GEANT4-simulated beam profile in EAR1 is shown in fig. 10, for the whole range of neutron energies. The results are consistent with measurements performed in various campaigns as summarized in ref. [13]. The simulated BIF for samples of various diameter is shown in fig. 11. In this case, experimental results do not allow for a meaningful comparison, since they are limited to a few tens of keV, where the BIF is approximately constant.
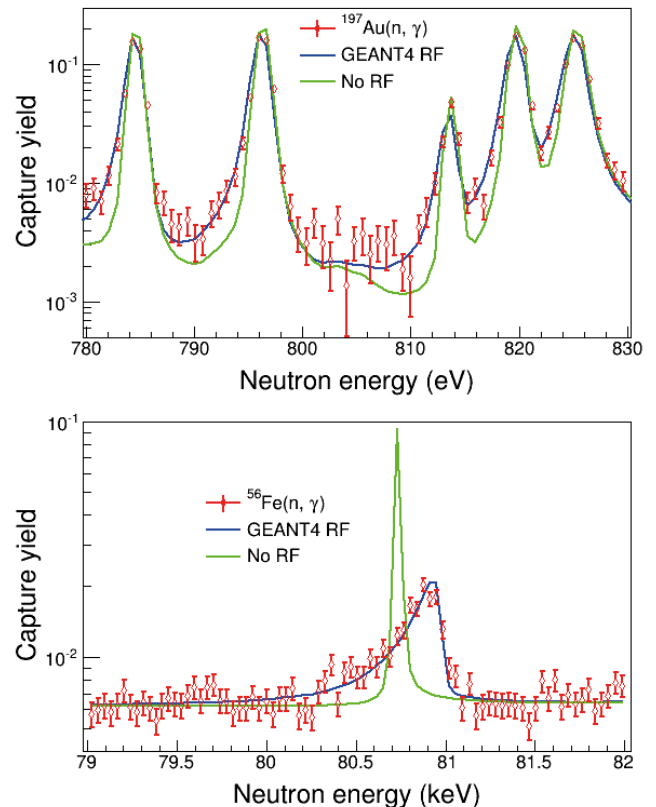

Fig. 9. Comparison between the simulated and the measured resonances in the well-known neutron capture cross section of ^{197}Au [37] (top) and ^{56}Fe (bottom).
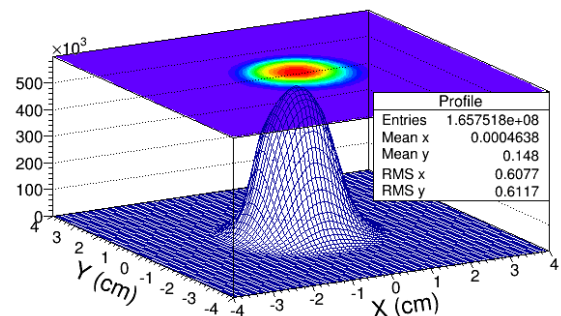

Fig. 10. Simulated neutron beam profile in EAR1 (at a distance of 185.2 m from the spallation target). The profile is obtained by propagating through the collimation system neutrons emerging from the target in GEANT4 simulations (see text for details on the propagation procedure). The RMS of the spatial distribution is about 0.61 cm, in agreement with the measured standard deviation [38].

3.4 The γ-ray flux

Apart from a vast variety of particles, photons are also copiously produced in the spallation process. Furthermore, the absorption of slow neutrons in the moderator and the surrounding material contributes to the photon flux. These in-beam photons cannot be removed from the beam, as it is done for charged particles by means of a suitable magnet, and thus represent an important source of background in all neutron capture experiments. Accordingly,
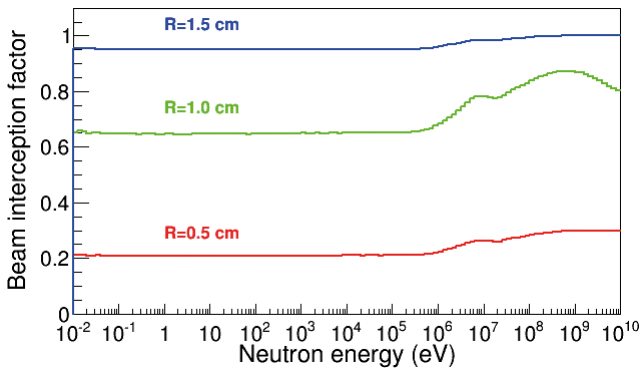
Fig. 11. Simulated fraction of the neutron beam intercepted by samples in EAR1 with radii of 0.5, 1.0 and 1.5 cm, as a function of the neutron energy.
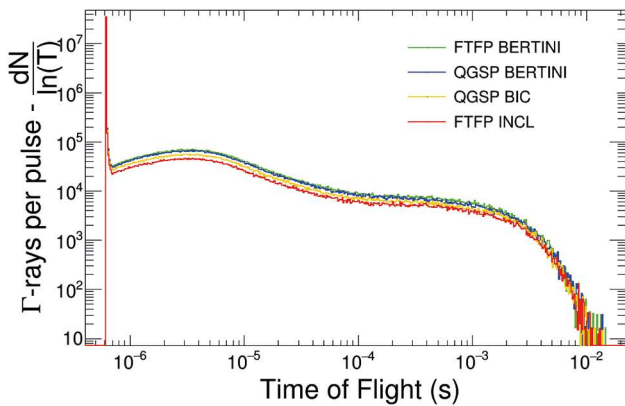

Fig. 12. Simulated total number of γ-rays per proton pulse produced in the spallation target and transported to EAR1 as a function of their arrival time in EAR1. Two components can be clearly distinguished: prompt γ-rays (at 615 ns) and delayed γ-rays beyond 1 μs.

Fig. 13. Energy distribution of simulated γ-rays produced in the spallation target assembly, for the prompt component (*i.e.* leaving the spallation target within a few ns from the start of the proton interaction), and for the delayed one (*i.e.* produced at later times).

simulations are very important for studies of the production and transport of photons in the spallation target and moderator, as well as for estimating the gamma flux in the experimental area. Figure 12 shows the flux of γ-rays, generated in the GEANT4 simulations of the n_TOF spallation target and transported to EAR1, as a function of their arrival time. Two different components can clearly be distinguished. The first one, the sharp peak starting at ~ 615 ns consists of prompt γ-rays emitted in high-energy interactions during the spallation process. Together with relativistic charged particles, this component constitutes the so called γ-*flash*, producing in most detectors a sharp signal, which is commonly used as time reference. The delayed component, beyond 1 μs, is made of γ-rays emitted from neutron inelastic and capture reactions taking place in the target-moderator assembly. The γ-ray energy distribution of these two components is shown in fig. 13 for different physics lists used in the simulations, illustrating the very different nature of the prompt and delayed γ-rays. According to the expectations, the simulated prompt γ-ray component is characterized by a hard spectrum, peaked at a few MeVs and extending to very high energies, reaching tens of GeV, since it arises from the nuclear reac-
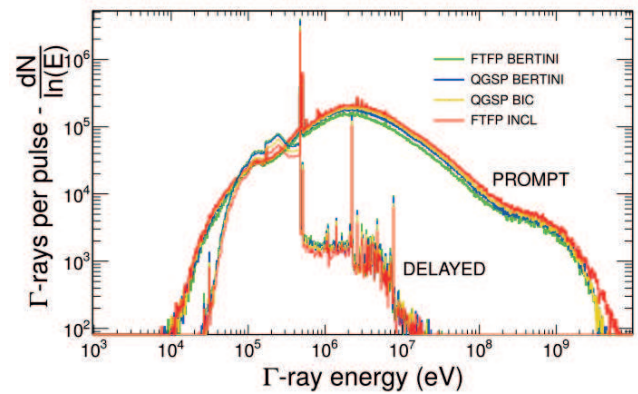
tions triggered by primary protons or mostly high-energy secondaries, including the fraction of energetic neutrons which do not undergo moderation. On the contrary, the delayed γ-ray component, mostly arising from thermal and epithermal neutrons captured in the moderator and the surrounding materials, is characterized by a soft spectrum and shows, among many others, the typical peaks at 478, 2200 and 7400 keV from capture in ^{10}B, ^{1}H and ^{27}Al. The production of γ-rays simulated with different physics lists shows an interesting pattern: the lists producing more delayed γ-rays are the ones including Bertini-type cascades, thus following the same pattern as neutron production, whereas the opposite happens for the prompt γ-ray yield. The correlation between the production of neutrons and delayed γ-rays can be understood on the basis of the already commented origin of the delayed γ-rays, generated by neutron interaction in the target/moderator assembly. On the other hand, prompt γ-rays mostly originate from π^0 decay, so that differences in the prompt γ-ray flux obtained with the different PLs are the consequence of different π^0 production probabilities in the various models. Furthermore, considering that the energy spent to produce this particle is at least partially removed from the energy available for neutron emission, π^0 production also has an effect on the neutron flux, thus explaining the anti-correlation between the neutron and prompt γ-ray fluxes observed in the simulations. The comparison between the simulated and measured neutron flux of the n_TOF facility could therefore provide an important indirect indication on the adequacy of π^0 production in various cascade models. The role of secondary pion production in spallation reactions, and their impact on neutron production, will be the subject of a forthcoming paper [39].

4 Conclusion

The spallation target/moderator assembly of the n_TOF facility at CERN has been simulated with GEANT4, in order to benchmark this tool for neutron generation and

transport in a wide energy range, as well as to extract detailed information on the characteristics of the neutron beam in EAR1. A detailed software replica of the spallation target with respect to the exact geometry and the materials involved has been implemented in the simulations. Neutrons emerging from the spallation target have been recorded and geometrically propagated through a reproduction of the collimation system. The simulated characteristics of the neutron beam in EAR1 at 185 m flight path have been compared with experimentally determined properties, for different choices of the PLs, in particular the intra-nuclear cascade and de-excitation models. The comparison of the neutron flux in EAR1 indicates that the best choice at present is the combination of the *INCL++* model with the native GEANT4 de-excitation model. This combination is able to reproduce very closely the energy distribution of the neutron beam, and predicts an absolute flux approximately 20% higher than the measured one. This difference can be taken as the level of systematic uncertainty of the simulations, related to the adopted models in GEANT4.

All other models predict a higher flux, with a possible explanation being related to differences in the treatment of π^0 production. In this respect, the measured flux of the n_TOF facility could provide a benchmark for optimizing this aspect in cascade models.

Although the use of the old version of the *ABLA* model, currently available in GEANT4, yields slightly worse results, it is possible that the newest version of this code, coupled with *INCL++*, may further improve the reliability of GEANT4 in simulations of spallation neutron sources. Other features of the neutron beam in EAR1, in particular the resolution function and the spatial beam profile, are well reproduced by the simulations, which therefore can be conveniently used when analysing data collected at n_TOF. The good agreement between the simulated and measured characteristics of the neutron beam in EAR1 indicate that GEANT4, with the proper choice of the physics list, can be used to reliably simulate spallation neutron sources for incident protons on lead at energies as high as 20 GeV, and, in our opinion, provide confidence for the ability of this code to accurately predict the neutron beam characteristics in a wide energy range.

References

1. F. Käppeler *et al.*, Rev. Mod. Phys. **83**, 157 (2011).
2. N. Colonna *et al.*, Energy Environ. Sci. **3**, 1910 (2010).
3. https://neutrons.ornl.gov/sns.
4. https://ntof-exp.web.cern.ch/ntof-exp/.
5. http://www.isis.stfc.ac.uk/.
6. http://j-parc.jp/index-e.html.
7. http://europeanspallationsource.se/.
8. http://csns.ihep.ac.cn/english/.
9. D.B. Pelowitz (Editor), *MCNPX User's Manual, Version 2.7.0*, Los Alamos National Laboratory report, LA-CP-11-00438 (2011).
10. A. Ferrari, P.R. Sala, A. Fassò, J. Ranft, CERN-2005-10 (2005) INFN/TC_05/11, SLAC-R-773.
11. S. Agostinelli *et al.*, Nucl. Instrum. Methods A **506**, 250 (2003).
12. P. Žugec *et al.*, Nucl. Instrum. Methods A **760**, 57 (2014).
13. The n_TOF Collaboration (C. Guerrero *et al.*), Eur. Phys. J. A **49**, 27 (2013).
14. The n_TOF Collaboration (M. Barbagallo *et al.*), Eur. Phys. J. A **49**, 156 (2013).
15. M.A. Cortés-Giraldo *et al.*, in preparation.
16. B. Andersson *et al.*, Nucl. Phys. B **281**, 289 (1987).
17. B. Nilsson *et al.*, Comput. Phys. Commun. **43**, 387 (1987).
18. S. Lo Meo *et al.*, Nucl. Phys. A **993**, 43 (2015).
19. A. Boudard *et al.*, Phys. Rev. C **87**, 014606 (2013).
20. D. Mancusi *et al.*, Phys. Rev. C **90**, 054602 (2014).
21. S. Leray *et al.*, J. Korean Phys. Soc. **59**, 791 (2011).
22. A. Kelić *et al.*, Report INDC(NDC)-0530 (2008) 181.
23. http://www-nds.iaea.org/spallations.
24. A. Boudard *et al.*, Phys. Rev. C **66**, 044615 (2002).
25. S. Pedoux, PhD thesis, University of Liège, Belgium (2011).
26. S. Pedoux, J. Cugnon, Nucl. Phys. A **866**, 16 (2011).
27. J.M. Quesada *et al.*, Prog. Nucl. Sci. Technol. **2**, 936 (2011).
28. A. Heikkinen *et al.*, J. Phys. Conf. Ser. **119**, 032024 (2008).
29. M.B. Chadwick *et al.*, Nucl. Data Sheets **107**, 2931 (2006).
30. M.B. Chadwick *et al.*, Nucl. Data Sheets **112**, 2887 (2011).
31. E. Mendoza, D. Cano-Ott, T. Koi, C. Guerrero, IEEE Trans. Nucl. Sci. **61**, 2357 (2014).
32. http://irfu.cea.fr/Sphn/Spallation/physlist.html.
33. GEANT4 Physics Reference and User Manuals at http://geant4.cern.ch.
34. The n_TOF Collaboration (G. Lorusso *et al.*), Nucl. Instrum. Methods A **532**, 622 (2004).
35. P. Schillebeeckx *et al.*, Nucl. Data Sheet **113**, 3054 (2012).
36. N.M. Larson, *Updated Users Guide for SAMMY: Multilevel R-matrix Fits to Neutron Data Using Bayes Equations, SAMMY Computer Code*, Report No. ORNL/TM-9179/R7, Oak Ridge National Laboratory, 2008.
37. C. Massimi *et al.*, Phys. Rev. C **81**, 044616 (2010).
38. J. Pancin *et al.*, Nucl. Instrum. Methods A **524**, 102 (2004).
39. D. Mancusi *et al.*, in preparation.